Supplementary Materials for

Altiratinib blocks *Toxoplasma gondii* and *Plasmodium falciparum* development by selectively targeting a spliceosome kinase

Christopher Swale[1†*], Valeria Bellini[1†], Matthew W. Bowler[2], Nardella Flore[3], Marie-Pierre Brenier-Pinchart[1], Dominique Cannella[1], Lucid Belmudes[4], Caroline Mas[5], Yohann Couté[4], Fabrice Laurent[6], Artur Scherf[3], Alexandre Bougdour[1*] and Mohamed-Ali Hakimi[1*]

*Corresponding author. Email: mohamed-ali.hakimi@univ-grenoble-alpes.fr (M.-A.H.); alexandre.bougdour@univ-grenoble-alpes.fr (A. B.); christopher.swale@univ-grenoble-alpes.fr (C. S.)

The PDF file includes:

Other Supplementary Material for this manuscript includes the following:

Table S3. Mass spectrometry-based characterization of the interactomes of PRP4K and PRP8.

Table S4. Statistics of crystallographic data.

Table S5. Description of T. gondii strains, plasmids and primers.

Supplementary Materials and Methods and references

Growth of *Cryptosporidium parvum* and RNA preparation. Hct-8 cells were grown in a T-75 flask (90% confluence) and infected with the *C. parvum* INRAE strain at a ratio of 5 oocysts per cell. Altiratinib was added to the treated flask at a concentration of 500 nM concentration. Four hours later, the flasks were washed to remove the oocysts and further incubated in presence of altiratinib until 11h post infection. All cells were collected and RNA extracted in Trizol solution for nanopore analyses.

In vitro* inhibition of *Eimeria tenella. Clec-213 chicken cell line was grown at 41°c in a CO2 incubator in DMEM F12 media supplemented with 10% SVF and 1% P/S. For EC50 determination, cells were seeded in 96 well plates and infected next day with Eimeria tenella freshly excysted sporozoites (Et-INRAE-nLuc strain) at a MOI of 1/1 for 5h followed by a washing to remove free sporozoites that did not infect the cells. 48h hours later, parasite development was assessed using the Nano-Glo luciferase assay (Promega). Values are sextuplicate for each drug concentration ± SEM.

Medium-throughput screening. The TargetMol (Boston, MA) compound library consists of 514 compounds (each as a 1 mM stock solution in DMSO). Primary screening was performed in white 96-well plates (3610, Corning ® *Costar* ®). The confluent HFFs monolayer was infected with 2000 RH NanoLuc parasites strain for 2 hours before the compounds were added at a final concentration of 5 µM in a final volume of 100 µl. The culture was incubated at 37°C for 48h. The medium was gently removed to add 50µl of PBS and measure the growth of the parasites (intra- and extracellular parasites were quantified) using the Nano-Glo® Luciferase Assay System, according to the manufacturer's instructions (Promega). Lysis was performed in the wells by adding 50 µL of Nano-Glo® Luciferase Assay Reagent with 1:50 dilution of Nano-Glo® Luciferase Assay Substrate. After 3 minutes of incubation, luminescence was measured using the CLARIOstar® (BMG Labtech) plate reader. The bioluminescence values of the uninfected host cells were used to determine the background signal. In parallel, to check the drugs effect on HFFs, infected and treated cultures were fixed with formaldehyde (3.7%) and stained with Hoechst 33258 at 2 µg/ mL in PBS for 10 min at room temperature. After three washes in PBS the nuclear florescence intensity was detected by the CLARIOstar® (BMG Labtech).

Measurement of EC_{50} for *Toxoplasma gondii* parasites. To measure the EC_{50} of *Toxoplasma gondii* parasites, confluent HFFs monolayer was infected with 2000 tachyzoites of RH parasites expressing the NLuc luciferase (RH NLuc) for 2h. After parasite invasion, each compound was added to the culture in

exponential concentrations. After 48h incubation at 37°C, the medium was replaced with 50 µl of PBS. The reading of luminescence was performed using the Nano-Glo® Luciferase Assay System according to the manufacturer's instructions (Promega). After 3 minutes of incubation, luminescence was measured using the CLARIOstar® (BMG Labtech) plate reader. EC_{50} values were determined using a non-linear regression analysis of normalized data and assuming a sigmoidal dose response. EC_{50} values for each compound represent the average of three independent biological replicates. Statistical analyses were performed using the one-way test ANOVA and GraphPad 8 software.

Measurement of CC50 for mammalian cells and determination of Selectivity Index. Human HFFs, ARPE-19, MCF7, and MDA-231 cell lines (Table S5) were plated for 1 hour in 96 well plates for 1h and incubated with exponential concentrations of the indicated compounds (THZ1 used as cytotoxic control) in a final volume of 100 µl. After 72h of culture, CellTiter-Blue Reagent® (Promega) (20 µl/well) was added directly to each well. Plates were then incubated at 37°C for 2 hours to allow cells to convert resazurin to resorufin before reading fluorescence (560(20) Ex/ 590(10) Em) with the CLARIOstar® (BMG Labtech) plate reader. The cytotoxicity concentration (CC50) of human cells was determined using nonlinear regression curve of the normalized data. CC_{50} values represent the average of two biological experiments. The Selectivity Index (SI) was determined by the average of the human CC_{50} divided by the average of the *T. gondii* EC_{50}. Mitochondrial toxicity assay was performed using the "Mitochondrial ToxGlo™ Assay" kit according to the manufacturer's instructions (Promega). Briefly, 10,000 human cell lines were plated in 96 well plates with DMEM serum and glucose free, supplemented with galactose (10 mM). After 3h of culture to allow cell adhesion, increasing concentrations of altiratinib (tested drug) and sodium azide (positive control for mitochondrial toxicity) or 800 µg/ml of digitonin (positive control for cell toxicity) were added. The cell culture was maintained at 37°C for 90 min to detect cell viability (cytotoxicity) by fluorescence and ATP production by luminescence using the CLARIOstar® (BMG Labtech) plate reader.

Reagents. The following primary antibodies were used in the immunofluorescence and immunoblotting: rabbit anti-TgGAP45 (gift from Pr. Dominique Soldati, University of Geneva), mouse anti-HA tag (Roche, RRID: AB_2314622), and rabbit anti-HA Tag (Cell Signaling Technology, RRID: AB_1549585). Immunofluorescence secondary antibodies were coupled with Alexa Fluor 488 or Alexa Fluor 594 (Thermo Fisher Scientific). Secondary antibodies used in Western blotting were conjugated to alkaline phosphatase (Promega) or horseradish peroxidase.

Immunofluorescence microscopy. *T. gondii* infecting HFF cells grown on coverslips were fixed in 3% formaldehyde for 20 min at room temperature, permeabilized with 0.1% (v/v) Triton X-100 for 15 min and blocked in Phosphate buffered saline (PBS) containing 3% (w/v) BSA. The cells were then incubated for 1 hour with primary antibodies followed by the addition of secondary antibodies

conjugated to Alexa Fluor 488 or 594 (Molecular Probes). Nuclei were stained for 10 min at room temperature with Hoechst 33258 at 2 μg/ mL in PBS. After four washes in PBS, coverslips were mounted on a glass slide with Mowiol mounting medium, and images were acquired with a fluorescence ZEISS ApoTome.2 microscope and images were processed by ZEN software (Carl Zeiss, Inc.).

Auxin induced degradation. Depletion of *Tg*PRP4K-AID-HA was achieved with 3-Indoleacetic acid (IAA, Sigma-Aldrich # 45533) as described (***1***). A stock of 500 mM IAA dissolved in 100% EtOH at 1:1,000 was used to deplete mAID-tagged proteins at a final concentration of 500 μM. Mock treatment consisted of an equivalent volume of 100% EtOH at a final concentration of 0.0789%, wt/vol. To monitor the degradation of AID-tagged proteins, parasites grown in HFF monolayers were treated with auxin, or ethanol alone, for different time intervals at 37℃. After treatment, parasites were harvested and analyzed by immunofluorescence or Western blotting. Complete elimination of *Tg*PRP4K parasites was successful after 10 hours of IAA treatment.

Plaque assays. Confluent HFFs were infected with freshly egressed tachyzoites before adding 0.1% DMSO or the indicated compounds. Cultures were grown at 37°C for 7 days, fixed, and stained with Coomassie blue staining solution (0.1% Coomassie R-250 in 40% ethanol and 10% acetic acid). For cytotoxicity assay, the parasites were incubated with different drugs or DMSO for 16 hours. After washing the cells, the cultures were left at 37°C for 3, 6 or 10 days before fixation and staining. The size of the plaques when present was measured using ZEN 2 lite software (Carl Zeiss, Inc.) and plotted using GraphPad Prism 8.

RNA-seq, sequence alignment, and variant calling. For each biological assay, a T175 flask containing a confluent monolayer of HFF was infected with RH wild-type or Altiratinib-resistant strains. Total RNAs were extracted and purified using TRIzol (Invitrogen, Carlsbad, CA, USA) and RNeasy Plus Mini Kit (Qiagen). RNA quantity and quality were measured by NanoDrop 2000 (Thermo Scientific). RNA-sequencing was performed as previously described (***2***), following standard Illumina protocols, by GENEWIZ (South Plainfield, NJ, USA). Briefly, the RNA quality was checked with the TapeStation System (Agilent Technologies, Palo Alto, California, USA), and Illumina TruSEQ RNA library prep and sequencing reagents were used following the manufacturer's recommendations using polyA-selected transcripts (Illumina, San Diego, CA, USA). The samples were paired-end multiplex sequenced (2 x 150 bp) on the Illumina Hiseq 2500 platform and generated at least 40 million reads for each sample. The quality of the raw sequencing reads was assessed using FastQC (http://www.bioinformatics.babraham.ac.uk/projects/fastqc/) and MultiQC (Ewels et al., 2016). The RNA-Seq reads (FASTQ) were processed and analyzed using the Lasergene Genomics Suite version 17 (DNASTAR, Madison, WI, USA) using default parameters. The paired-end reads were uploaded onto the SeqMan NGen (version 17, DNASTAR. Madison, WI, USA) platform for reference-based assembly

and variant calling using the *Toxoplasma* Type I GT1 strain (ToxoDB-46, GT1 genome) as reference template. The ArrayStar module (version 17, DNASTAR. Madison, WI, USA) was used for variant detection and statistical analysis of uniquely mapped paired-end reads using the default parameters. Variant calls were filtered to select variants present in coding regions with the following criteria: variant depth ≥ 30, Q call ≥ 60, and absent in the parental wild-type strain. Mutations were plotted on a Circos plot using Circa (OMGenomics.com). For the expression data quantification and normalization, the FASTQ reads were aligned in parallel to the ToxoDB-46 build of the *Toxoplasma gondii* GT1 genome (ToxoDB-46) using Subread version 2.0.1 (Liao et al., 2013) with the following options 'subread-align -d 50 -D 600 --sortReadsByCoordinates'. Read counts for each gene were calculated using featureCounts from the Subread package. Differential expression analysis was conducted using DESeq2 and default settings within the iDEP.92 web interface. Transcripts were quantified and normalized using TPMCalculator. The Illumina RNA-seq dataset generated during this study is available at NCBI GEO: **GSE193614** (https://www.ncbi.nlm.nih.gov/geo/query/acc.cgi?acc=GSE193614).

Plasmid construction. The plasmids and primers for gene of interest (GOI) used in this work are listed in Table S5. To construct the vector pLIC-GOI-HAFlag, the coding sequence of GOI was amplified using primers LIC-GOI-Fwd and LIC-GOI-Rev using *T. gondii* genomic DNA as template. The resulting PCR product was cloned into the pLIC-HF-dhfr or pLIC-mCherry-dhfr vectors using the Ligation Independent Cloning (LIC) cloning method. Twenty mers-oligonucleotides corresponding to specific GOI were cloned using Golden Gate strategy. Briefly, primers GOI-gRNA-Fwd and GOI-gRNA-Rev containing the sgRNA targeting GOI genomic sequence were phosphorylated, annealed and ligated into the pTOXO_Cas9-CRISPR plasmid linearized with BsaI, leading to pTOXO_Cas9-CRISPR::sgGOI. Just two transgenic components are needed to implement the auxin-inducible degron (AID) system, a plant auxin receptor called transport inhibitor response 1 (TIR1) and a POI tagged with an AID. We engineered a type I RHΔku80 and a type II lines of *T. gondii* to stably express Tir1 from Oryza sativa tagged with Ty and controlled by a promoter selected for a moderate expression of the chimeric protein. The plasmid *pModProm1-TiR1-TY1-3DHFR* (DNA sequence in Table S5 was DNA synthetized and then cloned in pUC57 simple by Genscript. The chimeric construct was inserted within the UPRT locus. We also created a pLIC vector containing a codon-optimized for *T. gondii* expression DNA block with the mAID from *Arabidopsis thaliana* auxin-responsive protein $IAA17^{E66\text{-}S133}$, as defined (*1*), in frame with a HA tag (Table S5).

***Toxoplasma gondii* transfection.** *T. gondii* strains were electroporated with vectors in cytomix buffer (120 mM KCl, 0.15 mM $CaCl_2$, 10 mM K_2HPO_4/ KH_2PO_4 pH 7.6, 25 mM HEPES pH7.6, 2 mM EGTA, 5 mM $MgCl_2$) using a BTX ECM 630 machine (Harvard Apparatus). Electroporation was performed in a 2 mm cuvette at 1.100V, 25 Ω and 25 µF. When necessary, the antibiotic (concentration) used for drug selection was chloramphenicol (20 µM), mycophenolic acid (25 µg/ml) with xanthine (50 µg/ml),

pyrimethamine (3 µM), or 5-fluorodeoxyuracil (10 µM). Stable transgenic parasites were selected with the appropriate antibiotic, single-cloned in 96 well plates by limiting dilution and verified by immunofluorescence assay or genomic analysis.

Chromatographic purification of *Tg*PRP4K- and *Tg*PRP8-containing complex. *T. gondii* extracts from RHΔ*ku80* or PruΔ*ku80* cells stably expressing HAFlag-tagged *Tg*PRP4K and *Tg*PRP8, were incubated with anti-FLAG M2 affinity gel (Sigma-Aldrich) for 1 hour at 4°C. Beads were washed with 10-column volumes of BC500 buffer (20 mM Tris-HCl, pH 8.0, 500 mM KCl, 20% glycerol, 1 mM EDTA, 1 mM DTT, 0.5% NP-40, and protease inhibitors). Bound polypeptides were eluted stepwise with 250 µg/ml FLAG peptide (Sigma Aldrich) diluted in BC100 buffer. For size-exclusion chromatography, protein eluates were loaded onto a Superose 6 HR 10/30 column equilibrated with BC500. Flow rate was fixed at 0.35 ml/min, and 0.5-ml fractions were collected.

Mass spectrometry-based Interactome analyses. Protein were stained with colloidal blue (Thermo Fisher Scientific) and gel bands excised before in-gel digestion using modified trypsin (Promega, sequencing grade). Resulting peptides were analyzed by online nanoliquid chromatography coupled to tandem MS (UltiMate 3000 RSLCnano and Q-Exactive HF, Thermo Scientific). Peptides were sampled on a 300 µm x 5 mm PepMap C18 precolumn and separated on a 75 µm x 250 mm C18 column (Reprosil-Pur 120 C18-AQ, 1.9 µm, Dr. Maisch) using 50-min gradients. MS and MS/MS data were acquired using Xcalibur (Thermo Scientific). Peptides and proteins were identified using Mascot (version 2.6) through concomitant searches against the *Toxoplasma gondii* database (ME49 taxonomy, version 30 downloaded from ToxoDB[47], the Uniprot database (*Homo sapiens* taxonomy, February 2019 download), a homemade database containing the sequences of classical contaminants, and the corresponding reversed databases. Trypsin was chosen as the enzyme and two missed cleavages were allowed. Precursor and fragment mass error tolerances were set at respectively 10 ppm and 25 mmu. Peptide modifications allowed during the search were: Carbamidomethyl (C, fixed), Acetyl (Protein N-term, variable) and Oxidation (M, variable). The Proline software (http://proline.profiproteomics.fr) was used to filter the results: conservation of rank 1 peptide-spectrum-matches (PSMs), PSM homology threshold p-value ≤ 0.01, PSM score ≥ 25, and minimum of 1 specific peptide per identified protein group. Proline was then used to perform a compilation and grouping of the protein groups identified in the different samples. The MS data have been deposited to the ProteomeXchange Consortium via the PRIDE partner repository with the dataset identifier PXD029455 and 10.6019/PXD029455. Proteins from the contaminant database were discarded from the final list of identified proteins. MS1-based label free quantification of the protein groups was performed using Proline to infer intensity-based absolute quantification (iBAQ) values that were used to rank identified Toxoplasma proteins in the interactomes.

Gene synthesis for recombinant expression of *Tg*PRP4K and *Pf*CLK3. Gene synthesis for all insect cell codon optimized constructs was provided by Genscript. The original *T. gondii Tg*PRP4K construct (aa 534-895) or *Pf*CLK3 (aa 336-692) were designed with non-cleavable C-terminal 6His tags and cloned between BamHI and HindIII sites into the pFastBac1 vector (Invitrogen). Point mutation variations of this initial construct were subsequently modified by Genscript from this original template. For the crystallization of *Tg*PRP4K, the cysteine 573 was mutated to a serine to prevent the formation of homomeric disulfide bond.

Generation of baculovirus. Bacmid cloning steps and baculovirus generation were performed using EMBacY baculovirus (kindly gifted by Imre Berger), which contains a YFP reporter gene in the virus backbone. The established standard cloning and transfection protocols setup within the EMBL Grenoble eukaryotic expression facility were used. While baculovirus synthesis (V0) and amplification (to V1) were performed with SF21 cells cultured in SF900 III media (Life Technologies), large-scale expression cultures were performed with Hi-5 cells cultured in Express-Five media (Life Technologies) and infected with 0,5% vol/vol of generation 2 (V1) baculovirus suspensions and harvested 72h post-infection.

Protein expression and purification. For purification, 3 cell pellets of approximately 800 mL of Hi-5 culture were each resuspended in 50 mL of lysis buffer (50 mM Tris pH 8.0, 500 mM NaCl and 4 mM β-mercaptoethanol (β-ME)) in the presence of an anti-protease cocktail (Complete EDTA free, Roche) and 1 ul benzonase (MERK Millipore 70746). Lysis was performed on ice by sonication for 3 min (30 sec on/ 30 sec off, 45° amplitude). After the lysis step, 5% of glycerol was added. Clarification was then performed by centrifugation for 1h at 12,000*g and 4°C. After that, 20 mM imidazole was added to the supernatant and incubated with 5 mL of Ni-NTA resin (Qiagen) with a stirring magnet at 4°C for 30 min. All further purification steps were then performed at room temperature. After flowing through the lysate, the resin was washed with 10 column volumes (cv) of lysis buffer containing 20 mM imidazole. Elution was then performed by increasing the imidazole content to 300 mM in a buffer system containing 200 mM NaCl, 50 mM Tris pH 7.5, 2 mM β-ME and 5% glycerol. Eluted fractions were pooled based on an SDS PAGE gel analysis and flown directly through a previously equilibrated (in 200 mM NaCl, 50 mM Tris pH 7.5, 2 mM β-ME and 5% glycerol) heparin column connected to an AKTA© pure system. After a 10 cv wash, the heparin was eluted using a 40 mL gradient reaching 2M NaCl. Finally, the sample was injected onto a SUPERDEX 200 increase 10/300GL (GE Healthcare) column running in 50 mM Tris pH: 7.5, 250 mM NaCl, 1 mM β-ME and 1% glycerol and the elution was monitored at 280 nm. Peak fractions were concentrated using a 30 kDa Amicon ultra (Sigma Aldrich) concentrator before being frozen in liquid nitrogen and stored long-term at -80°C.

Western blot. Briefly, ~10^7 cells were lysed in 50 µl lysis buffer (10 mM Tris-HCl, pH6.8, 0.5 % SDS [v/v], 10% glycerol [v/v], 1 mM EDTA and protease inhibitors cocktail) and sonicated. Proteins were separated by SDS-PAGE, transferred to a polyvinylidene fluoride membrane (Immobilon-P; EMD Millipore) by liquid transfer, and Western blots were probed using appropriate primary antibodies followed by alkaline phosphatase or horseradish peroxidase-conjugated goat secondary antibodies. Signals were detected using NBT-BCIP (Amresco) or enhanced chemiluminescence system (Thermo Scientific).

Thermal Shift Assay (TSA). The thermal stability of recombinant WT and mutants *Tg*PRP4K proteins in the presence or absence of altiratinib compound was performed in TSA buffer (400 mM NaCl, 50 mM Hepes, 1 mM $MgCl_2$ and 2 mM β-ME). Each assay tube contained a reaction mixture (final volume of 20µl) of recombinant PRP4K enzyme (0.170 mg/ml) and 100µM inhibitor or 1% dimethyl sulfoxide (DMSO) in TSA buffer. The reactions were incubated at increasing temperatures, 30°C, 33°C, 36 C°, 39°C, 42°C, 45°C, 48°C, 51°C, 54°C, 57°C, 60°C, 63°C, 66°C, 69°C, for 3 minutes and then centrifuged at 16000 xg for 25 minutes. The supernatant was collected to verify the presence of the recombinant PRP4K/CLK3 proteins by Western blot. Proteins were blotted as previously described and detected using Anti-polyHistidine-Peroxidase monoclonal antibody (Sigma-Aldrich # A7058) and signals were revealed using the Metal Enhanced DAB Substrate Kit, according to the manufacturer's instructions (Thermo Scientific # 34065). Band intensities were integrated using ImageJ and Tm values were determined using GraphPad prism. The assays were performed in a triplicate fashion.

Microscale thermophoresis (MST). MST measurements were performed using a NanoTemper Monolith NT.115 Green/Red instrument (NanoTemper Technologies). *Tg*PRP4K protein was labeled using the Monolith His-Tag Labeling Kit RED-tris-NTA 2nd Generation (NanoTemper Technologies) and spun down after labelling to remove potential aggregates. The labeled *Tg*PRP4K protein was adjusted to 100 nM with a buffer containing 30 mM HEPES (PH 7.5), 50 mM NaCl, 2% Glycerol, 1 mM β-ME and 1 mM MgCl2. A series of 16 1:2 dilutions of the ligands was prepared in pure DMSO to exclude any effect of DMSO on the assay. Subsequently, 1ul of ligand dilution was mixed with 9 ul of titration buffer after which 10 ul of PRP4K at 200 nM were added. Samples were placed in Premium capillaries (NanoTemper technologies) for measurements. Instrument parameters were set to 40% LED power and 40% MST power, signal integration was performed with MO Affinity Analysis software (NanoTemper Technologies) using the signal from an MST-on time at 1.5 sec after T-jump. Data from three independent titrations were merged and exported as mean Fnorm% values +/- SEM. Triplicate measurements were fitted with a 4-parameter non-linear curve to determine apparent Kds and uncertainty values and represented as average points within graphpad prism for the figure.

Kinase activity assays. Serial dilutions of altiratinib were prepared in pure dmso to exclude any DMSO effect on the assay. 1ul of this serial dilution (or pure dmso for the 0 concentration) was then added to 55 uL reaction mix consisting of 107 nM of *Tg*PRP4K, 22 uM of ATP, 22 uM of *Toxoplasma* PRP31 phosphorylation site peptide (GNETAGCGFSSSLTFTPI, synthetized by Genscript), 50 mM NaCL, 50 mM Tris pH 7.5, 2 mM β-ME, 2 % glycerol and 5 mM MgCl2. After mixing, the reactions were kept for 3h at 30°C in a thermocycler. Endpoint ATP content was revealed using the KinaseGlo®Plus by Promega using the kit protocol. Luminescence titrations were measured on the Clariostar (BMG Labtech) with a 10 second acquisition time within white 384 well plates. Raw luminescence data was then normalized for every *Tg*PRP4K condition with the lowest value (at titration point O) corresponding to 100% kinase activity. All titrations were performed in triplicate manner. Apparent IC50 determination was realized through a 4-parameter nonlinear inhibition curve fitting in GraphPad prism.

SEC-MALLS. All MALLS runs were performed using an S200 Increase SEC column (10/300 GL, GE Healthcare) running in a buffer system containing 50 mM Tris pH: 7.5, 250 mM NaCl, 1 mM β-ME . Sample injection and buffer flow were controlled by a Hitachi L2130 pump. The SEC column was followed by an L-2400 UV detector (Hitachi), an Optilab T-rEX refractometer (Wyatt technologies), and a DAWN HELEOS-II multi-angle light scattering detector (Wyatt technologies). Injections of 50 µL were performed using protein samples concentrated at a minimum of 4 mg.mL−1, a constant flow rate of 0.5 mL.min−1 was used. Accurate MALLS mass prediction was performed with the Astra software (Wyatt Technologies). The curves were plotted using Graphpad (Prism).

Crystallization with Altiratinib. For *Tg*PRP4K/Altiratinib co-crystal growth, *Tg*PRP4K at 2-5 mg/ml was incubated for 20 minutes with 400 µM of altiratinib prior to injection on an S200 column running 50 mM Tris pH 7.5, 250 mM NaCl, 1 mM β-ME and 1% glycerol. The eluted protein was then pooled and concentrated to 20 mg/ml. It should be noted that altiratinib generates a typical absorbance signature below 260 nm which increases with the concentration of the protein. Crystallization was setup using the hanging drop vapor diffusion method with *Tg*PRP4K/altiratinib mixed in a 1/1 ratio with 18% PEG 3350 and 0.18 M Potassium thiocyanate. Crystals appeared generally after 2 weeks. The crystals were harvested using Hampton nylon loops, cryo-protected in the mother liquor supplemented with 18-20% glycerol and flash frozen in liquid nitrogen.

Data collection and structure determination. X-ray diffraction data for *Tg*PRP4k/altiratinib crystals were collected by the autonomous beamline MASSIF-1 at the European Synchrotron Radiation Facility (ESRF) beamline MASSIF-1 (***3***, ***4***) using automatic protocols for the location and optimal centering of crystals (***5***). Strategy calculations accounted for flux and crystal volume in the parameter prediction for complete datasets. Diffraction was performed at 100K. Data collection was performed using XDS (***6***) while amplitude scaling/merging was handled by the Staraniso server (Global phasing LTD). Molecular replacement solutions were obtained with Phaser (***7***) (within Phenix) using the crystal structure of

human PRPF4B bound to rebastinib [Protein Data Bank (PDB) code: 6CNH] as a template, the initial solution was then improved through cycles of manual adjustment in Coot (***8***) and automated building in phenix autobuild (***9***). The Altiratinib geometry restraints were generated in phenix using *elbow*. Refinement was performed using Refmac5, phenix resolve or Buster (Global Phasing Ltd). Final pdb model corrections were performed using the pdb-redo server.

Differential splicing analysis. Splice correction, collapse, quantification and differential isoform representation was performed using the FLAIR pipeline (***10***) with standard parameters however keeping non-consistent isoforms after the correction stage. The difference splicing script was used to generate gtf track files and quantification histograms.

Intron retention quantification. Prior to counting retained introns the original gff files from eupadDB were processed using the Agat-conv (https://github.com/NBISweden/AGAT) program "agat_convert_sp_gff2gtf.pl". Introns were added to the gtf file with "agat_sp_add_introns.pl". A per transcript intron retention ratio was calculated by counting per transcript intron counts divided by standard transcript counts (+1) using htseq-count with the following input parameters parameters:

- "htseq-count -f bam -r name -s yes -i Parent -t intron -m intersection-nonempty" for retained introns per-transcript
- "htseq-count -f bam -r name -s yes -i ID -t transcript -m intersection-nonempty" for total transcripts

Subsequent merging treatment of count data was carried out in excel worksheets. The intron retention analysis was limited to spliced genes with a minimum of 2 transcripts. Intron retention values above 1 were excluded as these values are probably the consequence of mis-annoted genes. Final distributions of retained intron ratios were done in GraphPad Prism.

P. falciparum **EC50 determination.** EC50 values were obtained as previously described (***11***). Briefly, a range of 2-step serial dilutions of altiratinib (starting concentration 5 µM) and Dihydroartemisinin (DHA, starting concentration 50 nM) were used to assess the activity of the compounds. GraphPad Prism 8 was used to interpolate IC_{50} from three independent experiments run in triplicate. DHA and DMSO were used as positive and negative controls, respectively.

P. falciparum **treatment and harvesting for RNA extraction.** 3.10^9 trophozoite-stage parasites aged of 24- to 30-hours post-red blood cell invasion were treated for 8 hours with a concentration of 2.5 µM of altiratinib (corresponding to the EC_{90}) or 0.1% DMSO (vehicle). The concentration and incubation time chosen were checked previously for inducing no obvious growth phenotype. Parasites were then washed with RPMI (Gibco) and harvested using 0.15% saponin lysis of the surrounding red blood cell.

After thorough washing with PBS, RNA was extracted using the RNeasy mini kit (Qiagen) and sent for analysis. RNA was harvested in two independent experiments.

References

1. D. C. Farhat, M. W. Bowler, G. Communie, D. Pontier, L. Belmudes, C. Mas, C. Corrao, Y. Couté, A. Bougdour, T. Lagrange, M. A. Hakimi, C. Swale, A plant-like mechanism coupling m6A reading to polyadenylation safeguards transcriptome integrity and developmental gene partitioning in Toxoplasma. Elife. 10, e68312 (2021).

2. V. Bellini, C. Swale, M. P. Brenier-Pinchart, T. Pezier, S. Georgeault, F. Laurent, M. A. Hakimi, A. Bougdour, Target Identification of an Antimalarial Oxaborole Identifies AN13762 as an Alternative Chemotype for Targeting CPSF3 in Apicomplexan Parasites. iScience. 23, 101871 (2020)

3. M. W. Bowler, D. Nurizzo, R. Barrett, A. Beteva, M. Bodin, H. Caserotto, S. Delagenière, F. Dobias, D. Flot, T. Giraud, N. Guichard, M. Guijarro, M. Lentini, G. A. Leonard, S. McSweeney, M. Oskarsson, W. Schmidt, A. Snigirev, D. von Stetten, J. Surr, O. Svensson, P. Theveneau, C. Mueller-Dieckmann, MASSIF-1: a beamline dedicated to the fully automatic characterization and data collection from crystals of biological macromolecules. Journal of Synchrotron Radiation 22,1540–1547 (2015).

4. O. Svensson, S. Malbet-Monaco, A. Popov, D. Nurizzo, M. W. Bowler, Fully automatic characterization and data collection from crystals of biological macromolecules. Acta crystallographica. Section D, Biological crystallography 71, 1757–1767 (2015).

5. O. Svensson, M. Gilski, D. Nurizzo, M. W. Bowler, Multi-position data collection and dynamic beam sizing: recent improvements to the automatic data-collection algorithms on MASSIF-1. Acta Crystallographica Section D Structural Biology 74, 433–440 (2018).

6.W. Kabsch, XDS. Acta crystallographica. Section D, Biological crystallography 66, 125–132 (2010).

7. A. J. McCoy, R. W. Grosse-Kunstleve, P. D. Adams, M. D. Winn, L. C. Storoni, R. J. Read, Phaser crystallographic software. Journal of applied crystallography 40, 658–674 (2007).

8. P. Emsley, K. Cowtan, Coot: model-building tools for molecular graphics. Acta crystallographica. Section D, Biological crystallography 60, 2126–2132 (2004).

9. T. C. Terwilliger, R. W. Grosse-Kunstleve, P. V. Afonine, N. W. Moriarty, P. H. Zwart, L. W. Hung, R. J. Read, P. D. Adams, Iterative model building, structure refinement and density modification with the PHENIX AutoBuild wizard. Acta crystallographica. Section D, Biological crystallography 64, 61–69 (2008).

10. A. D. Tang, C. M. Soulette, M. J. van Baren, K. Hart, E. Hrabeta-Robinson, C. J. Wu, A. N. Brooks, Full-length transcript characterization of SF3B1 mutation in chronic lymphocytic leukemia reveals downregulation of retained introns. Nat Commun. 11, 1438 (2020).

11. F. Nardella, L. Halby, E. Hammam, D. Erdmann, V. Cadet-Daniel, R. Peronet, D. Ménard, B. Witkowski, S. Mecheri, A. Scherf, P. B. Arimondo, DNA Methylation Bisubstrate Inhibitors Are Fast-Acting Drugs Active against Artemisinin-Resistant Plasmodium falciparum Parasites. ACS Cent Sci. 6, 16-21 (2020).

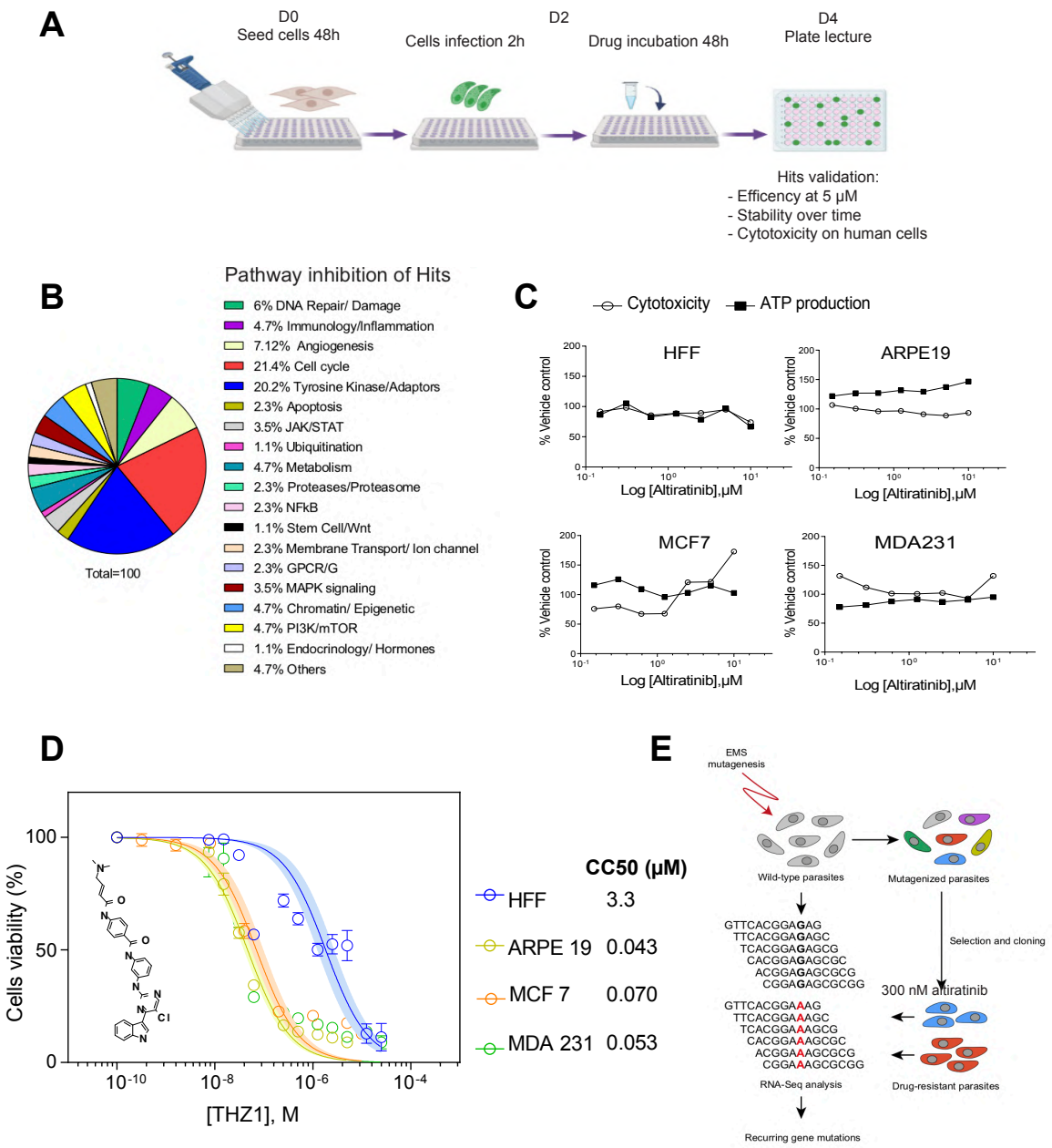

Fig. S1. Identification of altiratinib by a medium-throughput screening of an FDA-approved library. (**A**) Schematic overview of the workflow used to screen the library of 514-FDA approved compounds. Confluent HFFs were infected for 2 hours with tachyzoites of the *T. gondii* RH strain expressing the NanoLuc luciferase (RH Δ*ku80 UPRT::NLuc-P2A-EmGFP*). Each compound was then added to the culture at a concentration of 5 µM for 48h. After washing and incubation with furimazine substrate, luciferase activity was detected to select hits. Hits were further validated by testing their efficiency at 1 µM and checking stability over time or toxicity to the host cells. (**B**) Distribution of 84 hits by pathway inhibition. (**C**) Mitochondrial toxicity assay. Human cells were incubated with increasing concentrations of altiratinib, sodium azide (positive control for mitochondrial toxicity) or 800µg/ml of digitonin (positive control for cell toxicity). After 90 min, cell viability (cytotoxicity) was detected by fluorescence readout, while ATP production was measured by luminescence as indicated in the "*Mitochondrial ToxGlo™ Assay"* kit (Promega). Plots are representative of two biological replicates. (**D**) Dose-response curves of HFFs, ARPE-19, MCF7, and MDA231 cell lines in the presence of THZ1 compound. Human cells were plated out and incubated with increasing concentrations of the drug. After 72h, cell viability was determined using the "*CellTiter-Blue Assay"* kit (Promega) and cell cytotoxicity concentration (CC50) was calculated. The graph is representative of two different experiments performed in triplicate. The shaded error envelopes indicate 95% confidence intervals. On the right, CC50 values show the mean of two experiments. (**E**) Workflow used to map mutations that confer resistance to altiratinib in parasites.

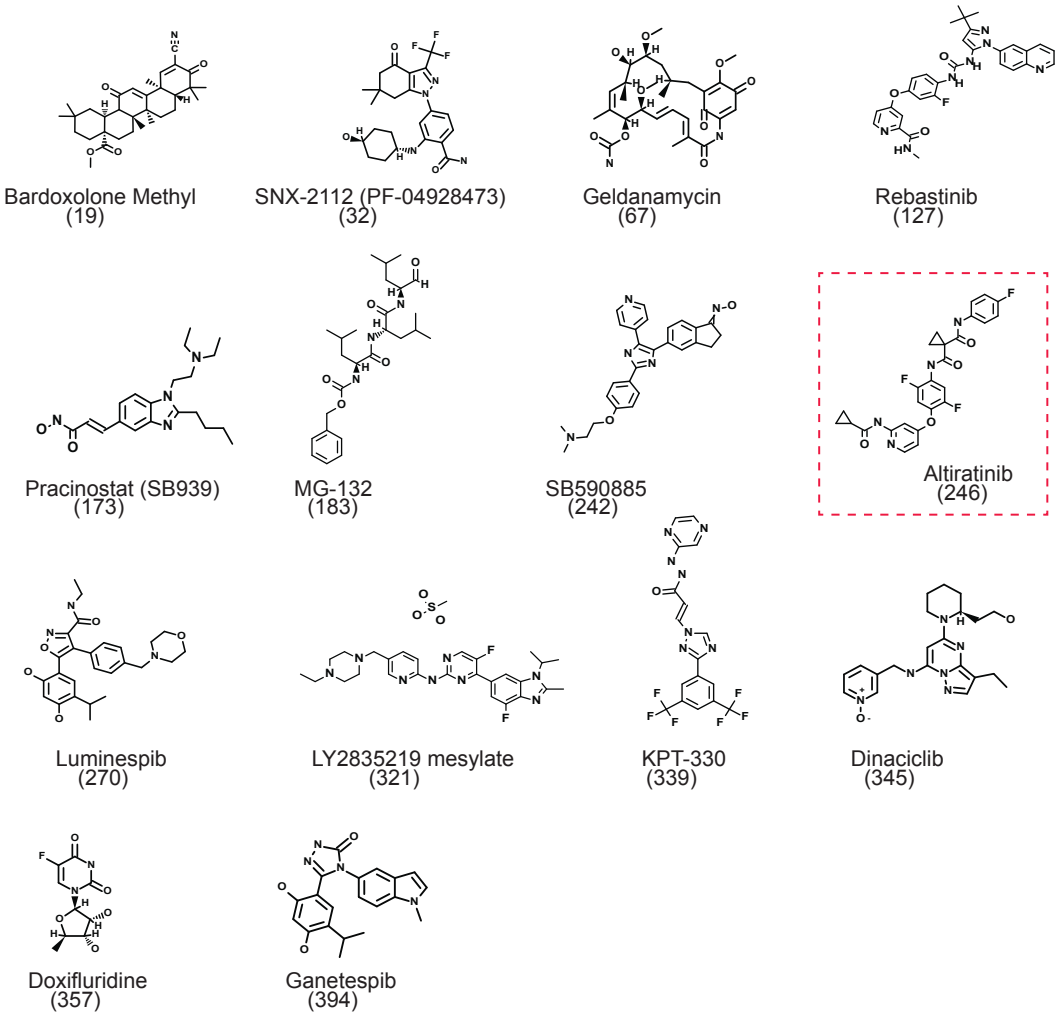

Fig. S2. Chemical structures of the 14 compounds selected for their efficacy in inhibiting the growth of T. gondii. The number under bracket corresponds to the number identifying the compound in the library described in Table S1.

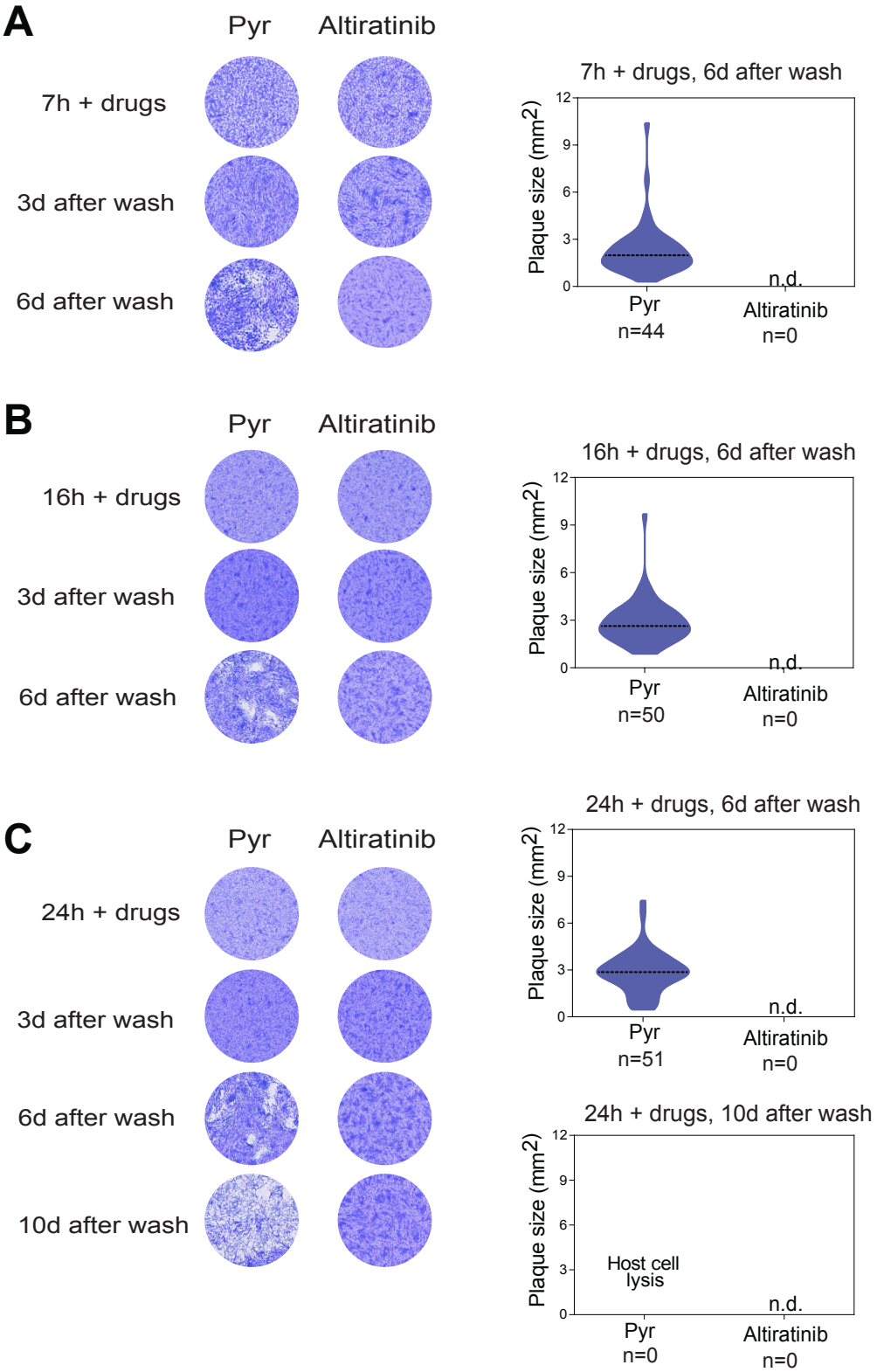

Fig. S3. Representation of *T. gondii* cytotoxicity after incubation with drugs. Confluent HFFs were infected with the strain RH WT (RH Δ*ku80 UPRT::NLuc-P2A-EmGFP*) and incubated with 1 µM of pyrimethamine or 300nM of altiratinib for 7 (**A**), 16 (**B**) or 24 hours (**C**). After 3, 6 or 10 days, the drugs were washed out and the cells were stained with Coomassie blue to detect the presence of plaques. Graphs show the size of visible plaques in each condition. n.d., not detected. Statistical analyses were performed using Mann-Whitney test (One-way ANOVA).

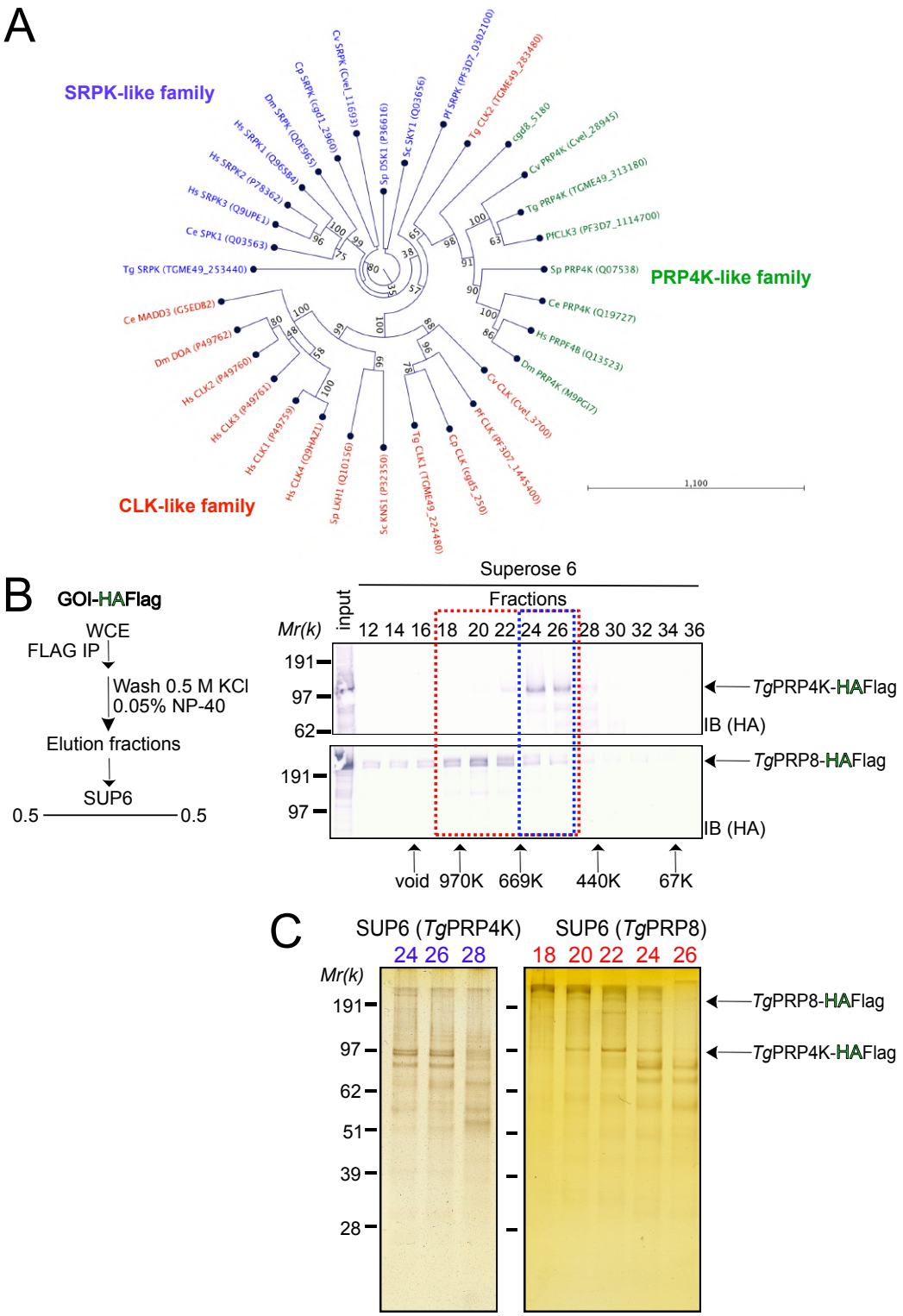

Fig. S4. Origin and interactome of *Tg*PRP4K. (**A**) Phylogenetic analysis of CLK-, PRP4K- and SRKP-like families. The unrooted phylogenetic tree was inferred from the kinase domain alignment. The tree was computed with the neighbor-joining algorithm, based on an HMM multiple alignment. The bootstrap values are shown in blue. The reliability of branching was assessed by the bootstrap resampling method using 1000 bootstrap replicates. (**B** and **C**) Size-exclusion chromatography of PRP4K- and PRP8-containing complexes after Flag-affinity selection. The fractions were analysed using western blots to detect PRP4K- or PRP8–HAFlag (anti-HA antibodies) (**B**) and on silver-stained SDS–PAGE gels (**C**).

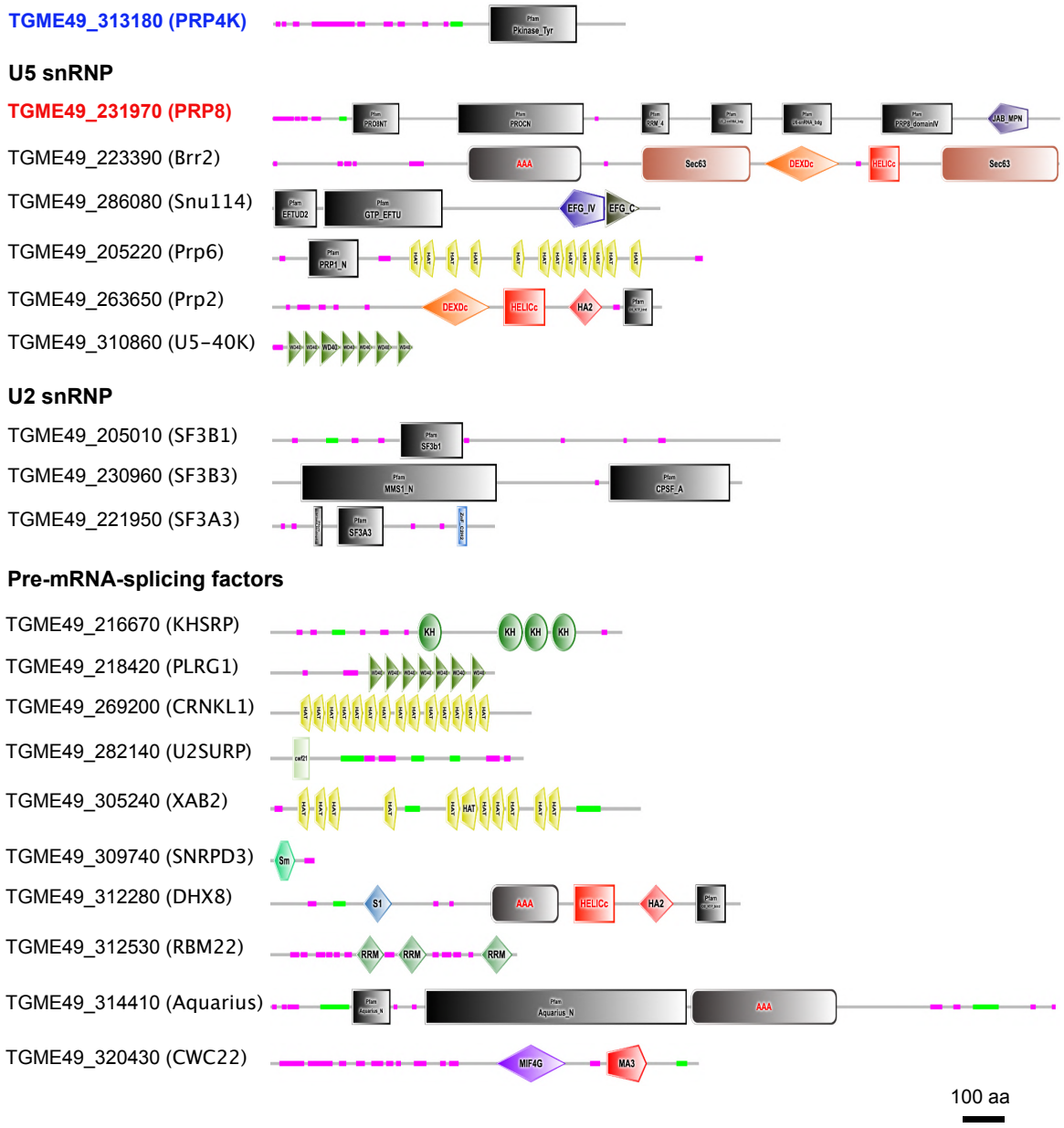

Fig. S5. Domain architectures of proteins purified together with PRP4K and PRP8. Representative domain architectures of T. gondii PRP4K and PRP8 partners identified by mass spectrometry-based proteomics (Table S3) are shown. Domains were predicted by SMART and PFAM.

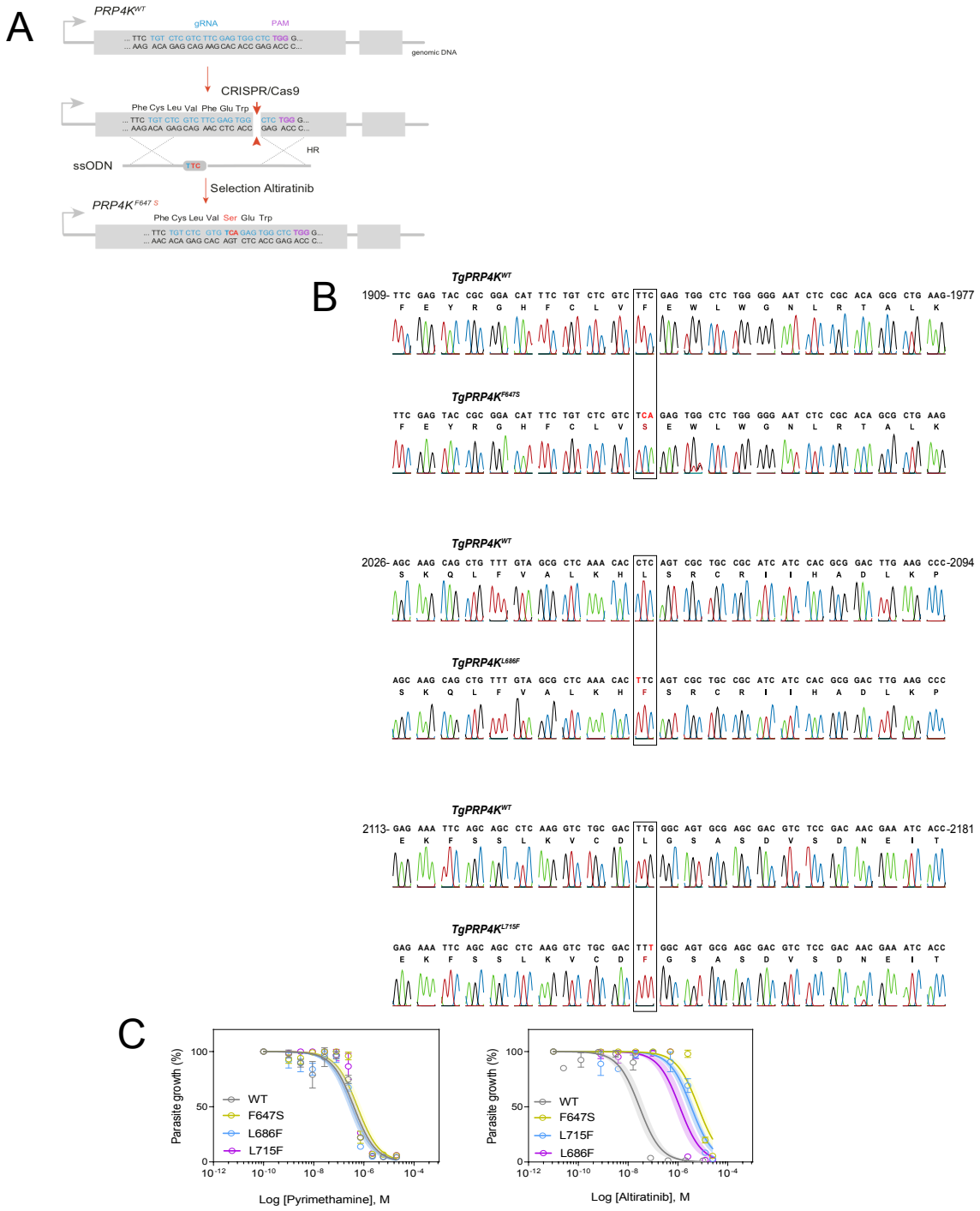

Fig. S6. Identification and validation of the molecular target *Tg*PRP4K. (**A**) Strategy for introducing point mutations into *T. gondii* parasites. Focus on the *Tg*PRP4K locus and CRISPR/Cas9-mediated homology-directed repair with single-stranded oligo DNA nucleotides (ssODNs) carrying nucleotide substitutions (red letters). After homologous recombination (HR) events, the *Tg*PRP4K recombinant parasites were selected with altiratinib. The engineered parasites were then validated by Sanger sequencing. (**B**) Sanger chromatograms validating *TgPRP4K* gene editing. Indicated are the nucleotide positions relative to the ATG start codon on the genomic DNA. **(C)** Dose–response curves for inhibition of *T. gondii* growth in response to increasing concentration of the indicated compounds. Confluent HFF monolayer were infected with WT and the engineered *Tg*PRP4K mutant strains expressing the NanoLuc luciferase. Data are presented as mean ± standard deviation (SD) of n=3 technical replicates from a representative experiment out of at least two independent biological assays. Shaded error envelopes depict 95% confidence intervals.

A

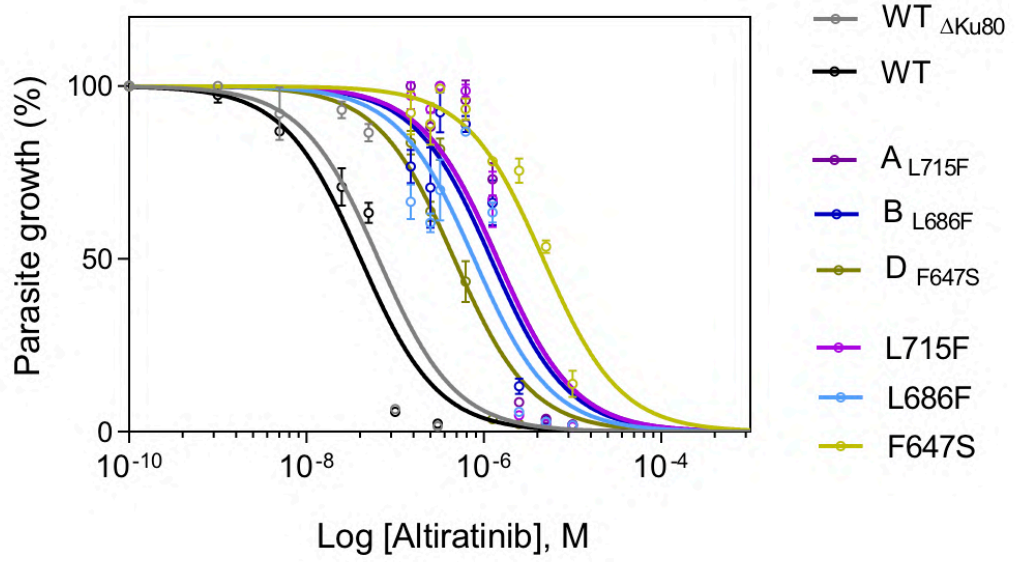

B

	Mutagenized parasite lines				Edited parasite lines			
Parasite strain	WT	A *L715F*	B *L686F*	D *F647S*	WT (ΔKu80)	L715F	L686F	F647S
Altiratinib EC_{50} (μM)	0.041	1.4	1.2	0.463	0.064	1.4	0.774	4.6

Fig. S7. Comparison of altiratinib resistance in EMS-mutagenized and CRISPR/Cas9-edited lines. (**A**) Dose-response curves for inhibition of T. gondii growth in response to increasing concentration of altiratinib. Confluent HFF monolayers were infected with EMS-mutagenized lines A (*Tg*PRP4K^{L715F}), B (*Tg*PRP4K^{L686F}), and D (*Tg*PRP4K^{F647S}), as well as with engineered *Tg*PRP4K mutant strains and parental strains RH^{WT} and RHΔ*ku80* (RH Nluc), respectively. Note that the NLuc-P2A-EmGFP reporter DNA construct was introduced into the *UPRT* locus of each mutagenized lines as described previously (Bellini *et al.,* 2020). Data are presented as mean ± standard deviation (SD) of n=3 technical replicates. (**B**) Table summarizing EC_{50} values for altiratinib determined by nonlinear regression analysis for the indicated strains.

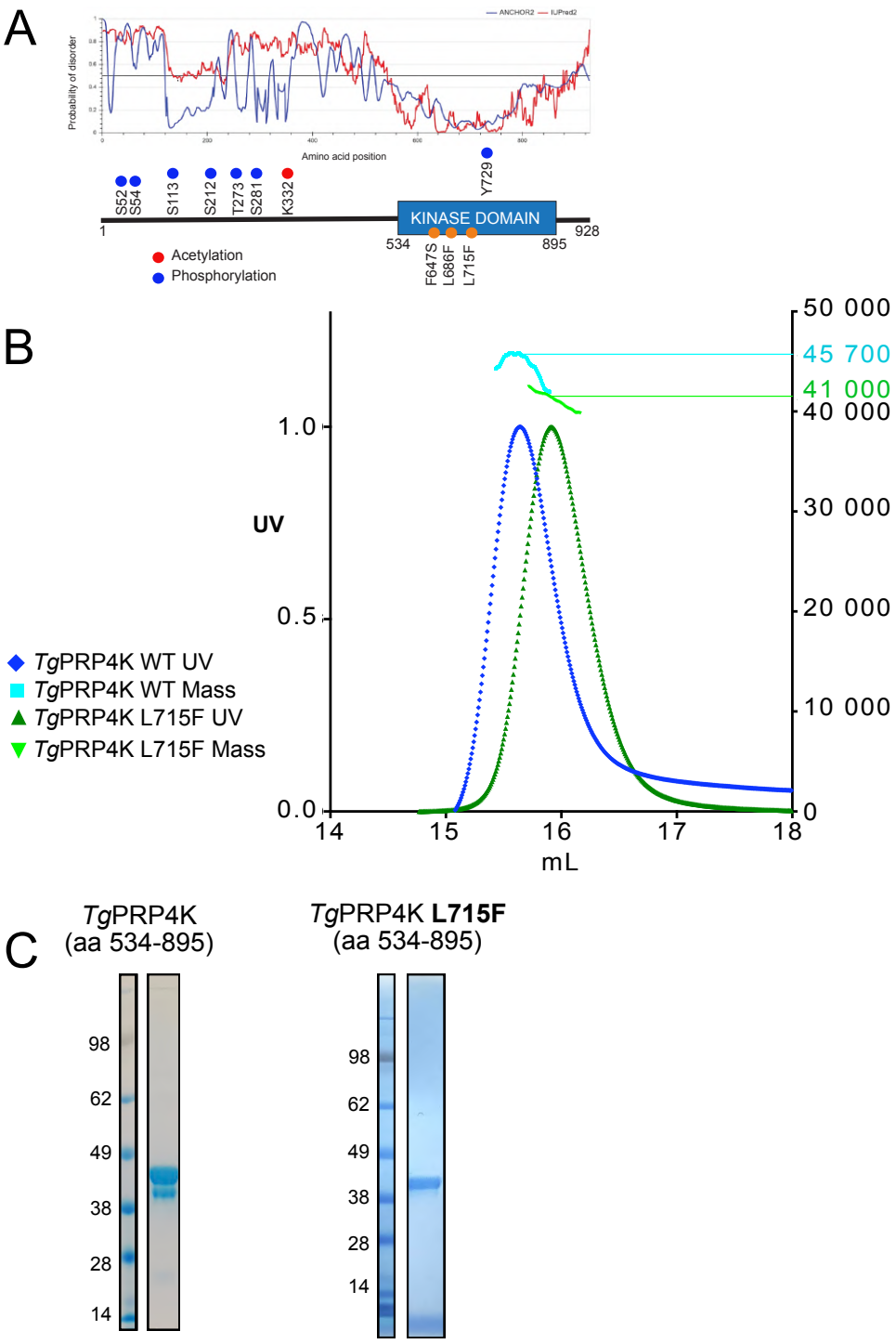

Fig. S8. Insect-cell recombinant expression of *Tg*PRP4K. (**A**) PRP4K full protein organization. IUpred disorder propensity prediction is shown above a linear schematic representation of the polypeptide chain. Phosphorylated and acetylated residues (data extracted from ToxoDB.org) are highlighted in blue and red respectively. (**B**) SEC-MALLS measurement of *Tg*PRP4K sample homogeneity. UV(280nm) absorbance chromatogram of insect cell purified WT (in blue) or L715F mutant (in green) *Tg*PRP4K (534-895) combined to a mass calculation as a scatter plot with the Y axis (in KDa) on the right when run on a S200 increase column. (**C**) SDS PAGE gel of recombinantly produced PRP4K. WT (left) and L715F (right) purified protein analysed a NuPage 5-12% Bis-Tris gel run in MES buffer and colored with Coomassie blue. The indicated numbers correspond to protein marker mass in kDa.

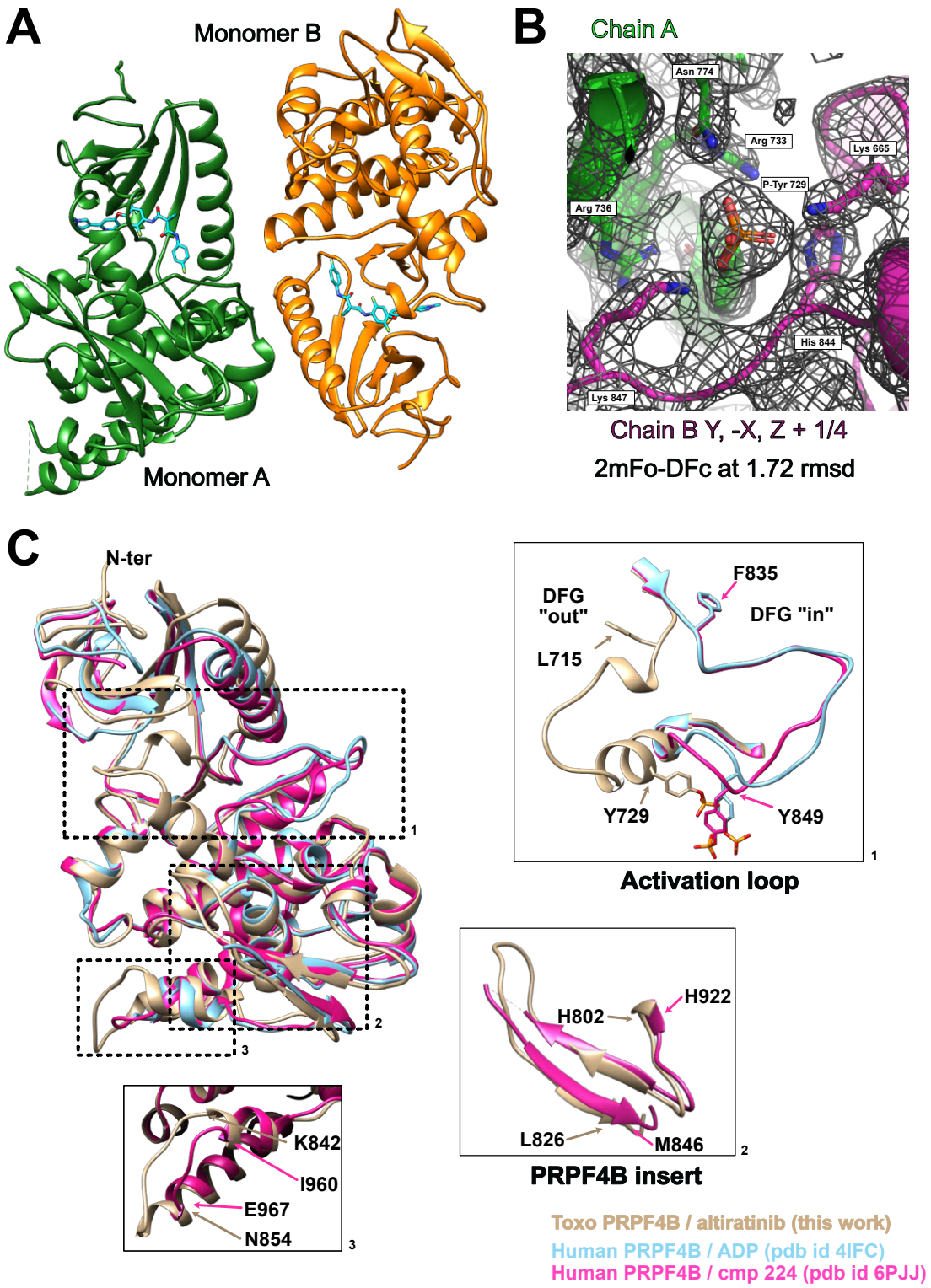

Fig. S9. Crystal structure specificities of *Tg*PRP4K. (**A**) Crystallographic dimerization of *Tg*PRP4K. Cartoon representation of chain/monomer A and B colored green and orange respectively. Altiratinib is displayed as sticks in cyan. (**B**) Phosphotyrosine 729 mediated crystal contacts. Cartoon and stick representation of the phosphotyrosine and interaction side chains from homo-monomeric and symmetry related molecules. 2mFo-DFc electron density is represented at a rmsd of 1.72. This specific representation was done using pymol. (**C**) Structural conservation of *Tg*PRP4K compared to the human *Hs*PRPF4B. Structural alignment shown in a cartoon fashion between *Tg*PRP4K bound to altiratinib (tan), ADP bound *Hs*PRPF4B (sky blue) and *Hs*PRPF4B (magenta) bound to cmp 224. Certain regions are shown enlarged for more detail.

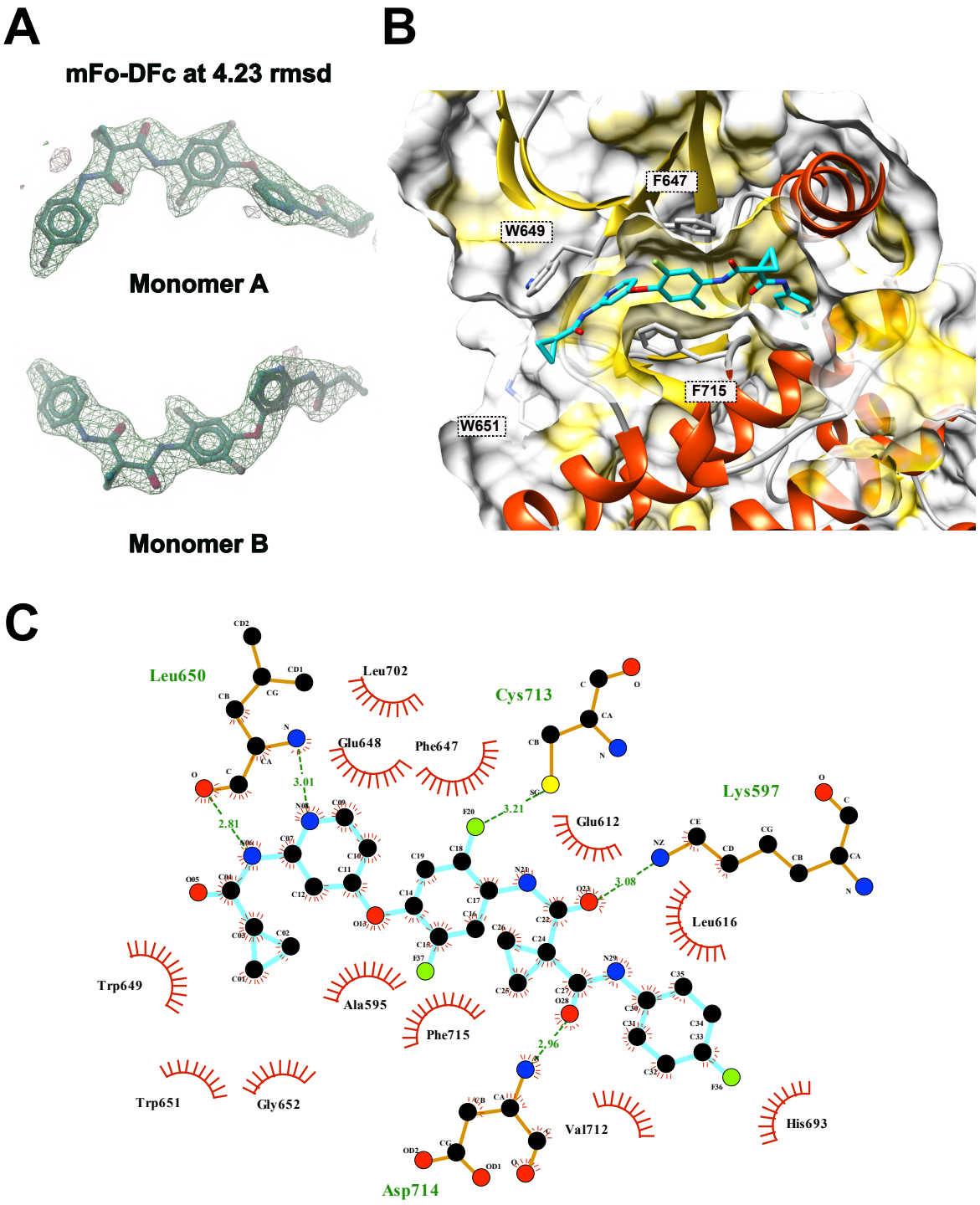

Fig. S10. Altiratinib binding site and interaction network. (**A**) Altiratinib omit map. Altiratinib mFo-DFc omit map (generated in coot) at 4.2 rmsd showing electron density as a green/grey mesh and the altiratinib stick structure in green. (**B**) ATP and allosteric pocket binding of altiratinib. Cartoon representation combined with a surface and hydrophobic attribute coloring (in yellow). Notable side chains involved in hydrophobic interactions are displayed as stick side chains. (**C**) Ligplot schematic 2D representation of all residues interacting with altiratinib. Charged interactions are displayed as green dotted lines whereas hydrophobic interactions are shown with red curved-in combs.

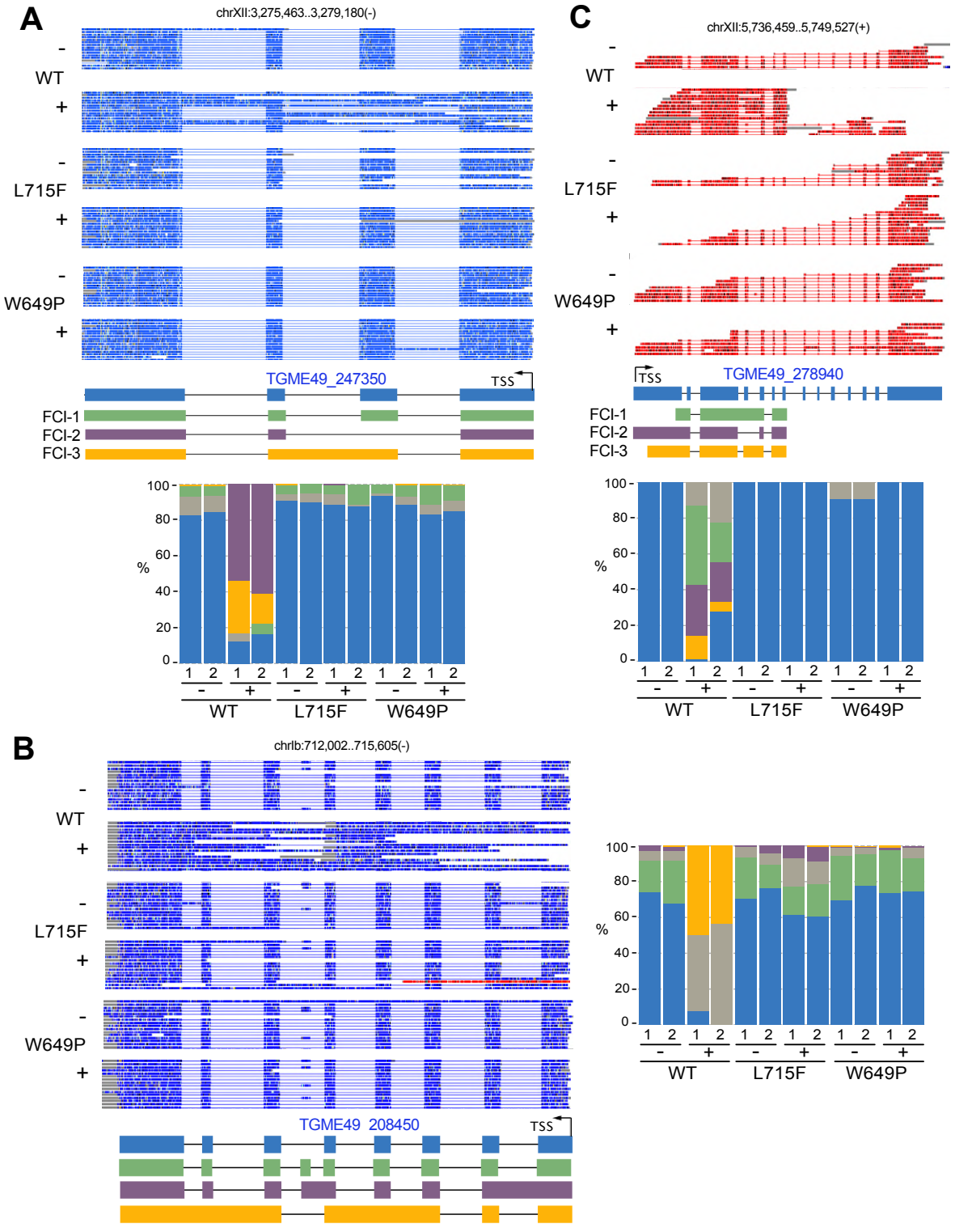

Fig. S11. DRS examples of altiratinib induced splicing defects in *Toxoplasma gondii*. FLAIR analysis of *TGME49_247350* (**A**), TGME49_208450 (**B**) and *TGME49_278940* (**C**) loci. Standard annotation and FLAIR collapsed isoforms (FCI) are shown schematically for all panels under a sample view of 15 reads per condition. Sense and antisense reads are colored red and blue, respectively. Below the FCI representation is an isoform quantification histogram showing duplicate measurements in each WT/L715F/W649P and untreated (-) or treated (+) condition. The color code is the same as for the above FCI, grey histograms represent minor isoforms that are not schematically represented.

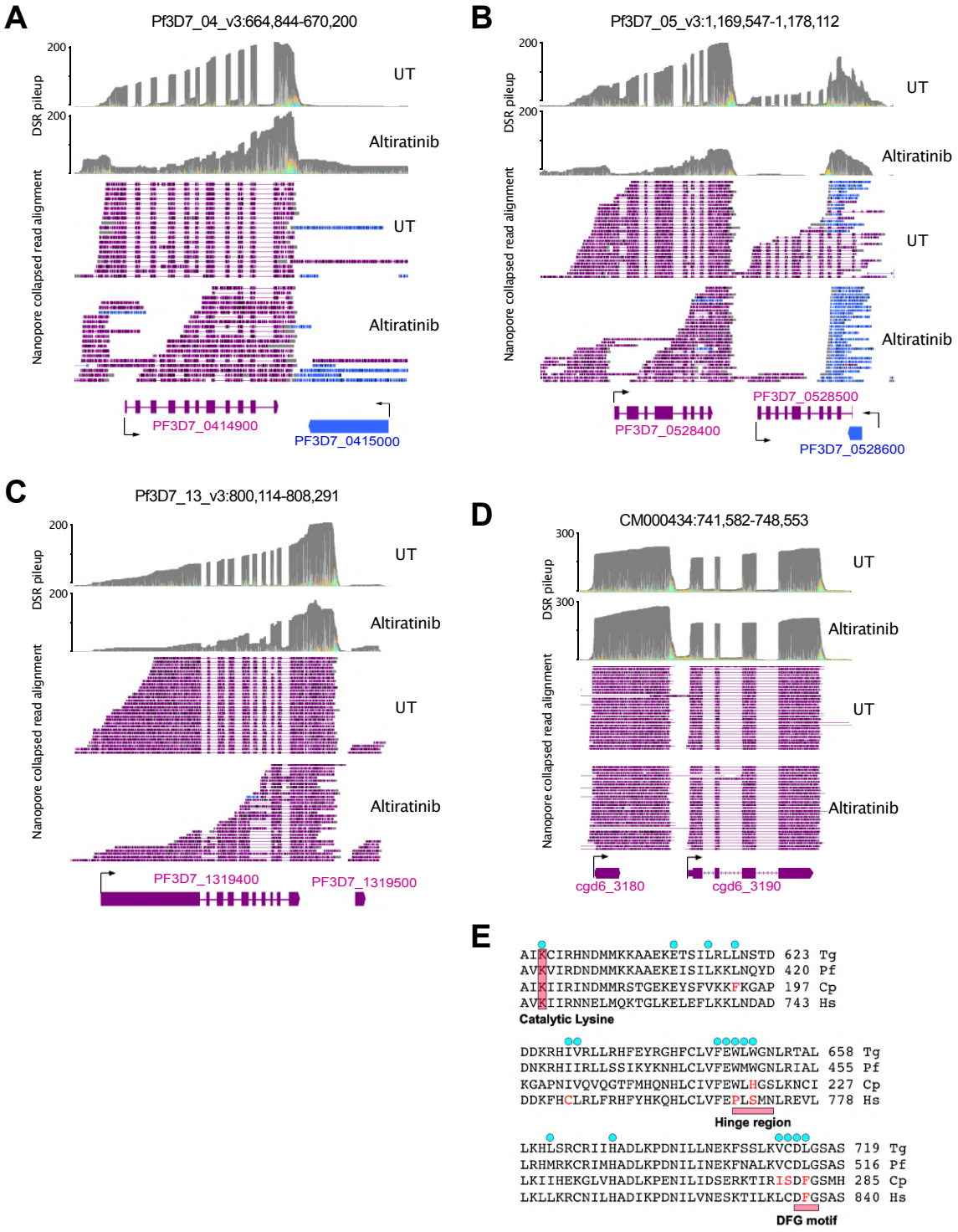

Fig. S12. DRS examples of altiratinib treatment on *Plasmodium falciparum* and *Cryptosporidium parvum*. FLAIR analysis of *PF3D7_0414900* (**A**), *PF3D7_0528400* (**B**), *PF3D7_1319400* (**C**) and *PF3D7_* loci in *Plasmodium falciparum* as well as the *cgd6_3190* loci (**D**) in *Cryptosporidium parvum*. Standard annotation and FLAIR collapsed isoforms (FCI) are shown schematically for all panels under a sample view of 15 reads per condition. Sense and antisense reads are colored purple and blue, respectively. Below the FCI representation is an isoform quantification histogram showing duplicate measurements in untreated (-) or treated (+) condition. The color code is the same as for the above FCI, grey histograms represent minor isoforms that are not schematically represented. (**E**) Sequence alignment of the *Tg*PRP4K binding regions of altiratinib compared to PRP4K/CLK3 orthologs of *Plasmodium falciparum* (*Pf*), *Cryptosporidium parvum* (*Cp*) and *Homo sapiens* (*Hs*). Key regions are highlighted by pink rectangles, altiratinib interacting amino acids from *Tg*PRP4K are shown by cyan circles, while divergent residues at the same position in the orthologs *of Cp* and *Hs* are shown in red.

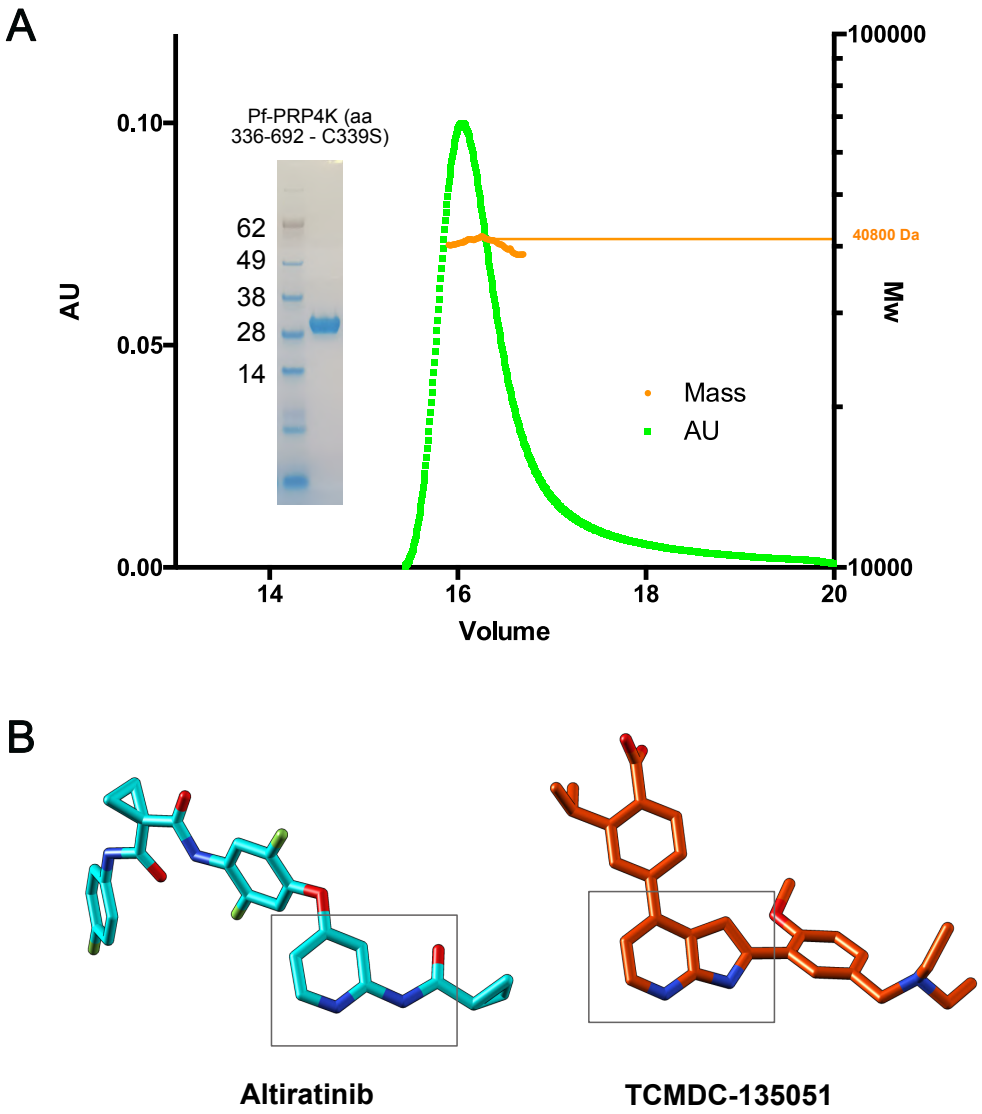

Fig. S13. Biochemistry of recombinant PfPRP4K and chemical structure comparison of Altiratinib and TCMDC-135051. (**A**) SEC-MALLS chromatogram of homogeneity of *Pf*PRP4K sample. UV (280nm) absorbance chromatogram of insect cell-purified *Pf*PRP4K (aa 336-692 with the C339 mutated to a S) combined to a mass calculation as a scatter plot with the Y axis (in kDa) on the right when run on a S200-increase column. Next to the chromatogram is a NuPAGE 4-12% gel of the same purified sample run in MES and stained with Coomassie blue. The numbers shown correspond to the marker mass in kDa. (**B**) Chemical structures of altiratinib (cyan) and TCMDC-135051 (orange) shown in a stick representation. The overall similarity is low, with the exception of the 7-azaindole scaffold of TCMDC-135051 which resembles the carbonylamino group connecting a pyridine ring of altiratinib.

Legend for Table S1 to S5

Table S1. Table describing the compound library and the selected molecules. The 514 compounds in the TargetMol© FDA-approved compound library, the 75 hits, and the 14 selected molecules are each described in a separate sheet.

Table 2. RNA-Seq Analysis of the EMS-Induced Drug-Resistant Lines of *T. gondii*. Mutations found in candidate genes by RNA-sequencing analysis of altiratinib-resistant mutants. Amino acid substitutions with corresponding codons shown in parentheses are indicated for each *T. gondii*-resistant mutant strain. The table includes the RNA-seq report, *T. gondii* transcripts (TPM), all variants, coding region variants, filtered variants in clones A to F, data used in Circos plot are shown in separate spreadsheets.

Table S3. Mass spectrometry-based characterization of the interactomes of PRP4K and PRP8. *Tg*PRP4K- and *Tg*PRP8-containing complexes were purified by affinity using FLAG tagging and subjected to size exclusion chromatography. Proteins present in the different eluted fractions were pooled and separated by SDS-PAGE. For *Tg*PRP4K, two lanes were analyzed with pools of fractions 24 and 26, and fractions 28 and 30. For *Tg*PRP8, three lanes were analyzed with fractions 14, 16 and 18, fractions 20 and 22, and fractions 24 and 26 (see below). The bands of interest in each lane, marked with arrows below, were excised and analyzed using MS-based proteomics. The parasite proteins identified and quantified in each band of the *Tg*PRP4K- and *Tg*PRP8-containing complexes are listed in the following tables.

Table S4. Statistics of crystallographic data.

Table S5. Description of *T. gondii* strains, plasmids and primers. List of *T. gondii* parasite lineages as well as plasmids used in this work. Primers used in this work are also listed.